

## Blend Cellulose Acetate Butyrate Membrane with Molecular Weight 12,000, 30,000 and 65,000 for CO<sub>2</sub>/N<sub>2</sub> Separation

Wong Shei Ming,<sup>1</sup> Zeinab Abbas Jawad,<sup>2\*</sup> Arwa Sulaiman,<sup>2</sup> and Chew Thiam Leng<sup>3,4</sup>

<sup>1</sup>Department of Chemical and Energy Engineering, Faculty of Engineering and Science, Curtin University Malaysia, 250 CDT, 98009 Miri, Sarawak, Malaysia

<sup>2</sup>Department of Chemical Engineering, College of Engineering, Qatar University, P.O. Box 2713, Doha, Qatar

<sup>3</sup>Department of Chemical Engineering, Faculty of Engineering, Universiti Teknologi PETRONAS, 32610 Seri Iskandar, Perak, Malaysia

<sup>4</sup>CO<sub>2</sub> Research Centre (CO2RES), Institute Contaminant Management, Universiti Teknologi PETRONAS, 32610 Seri Iskandar, Perak, Malaysia

\*Corresponding author: zjawad@qu.edu.qa

Published online: 30 April 2024

To cite this article: Ming, W. S. et al. (2024). Blend cellulose acetate butyrate membrane with molecular weight 12,000, 30,000 and 65,000 for CO<sub>2</sub>/N<sub>2</sub> separation. *J. Phys. Sci.*, 35(1), 35–51. <https://doi.org/10.21315/jps2024.35.1.4>

To link to this article: <https://doi.org/10.21315/jps2024.35.1.4>

**ABSTRACT:** *The demand for energy has been increasing gradually due to the rapid growth of the global economy. The emission of greenhouses gases (GHGs) especially, carbon dioxide (CO<sub>2</sub>), which is a major greenhouse gas, has contributed to the global warming issue. Therefore, to reduce emissions and eliminate the serious consequences, membrane separation technology was introduced as an alternative option that has high CO<sub>2</sub> separation efficiency. It requires lower energy consumption, lower capital costs and it is commercial and environmentally friendly. Most importantly, it is easy to operate. In this study, the blend cellulose acetate butyrate (CAB) membrane was synthesised from the CAB polymers using the wet-phase inversion method with molecular weights of 12,000:30,000:65,000 in the ratio of 1:2:2, respectively. The blend CAB membrane casted at 250 µm (M2) was the best performing membrane among all the membranes due to its relatively high CO<sub>2</sub> gas permeance and the highest CO<sub>2</sub>/N<sub>2</sub> selectivity, which were 7,560.80 ± 20 GPU and 1.5319 ± 0.05, respectively. The fabricated CAB membrane was then characterised by using the Attenuated Total Reflectance Fourier-Transform Infrared Spectroscopy (ATR-FTIR) and surface contact angle. It showed strong stretching bands around 1,044.07 cm<sup>-1</sup>, 1,226.25 cm<sup>-1</sup> and 1,744.04 cm<sup>-1</sup>, which indicated a single bond C-O and carboxyl group (C=O). The higher the hydrophobicity of the membrane, the stronger the affinity for CO<sub>2</sub> molecules. In this case, the contact angle of the membrane*

*casted at 150 μm (M1) was 120.46<sup>0</sup>, which was the highest. This newly synthesised CAB membrane is expected to benefit major industries by its cost effective and high energy saving properties. Most importantly, the gas separation efficiencies are better than the current technologies.*

**Keywords:** greenhouse gases, carbon dioxide separation, blend cellulose acetate butyrate membrane, CO<sub>2</sub>/N<sub>2</sub> separation, different molecular weight

## 1. INTRODUCTION

As a result of rapid growth and development of the world economy, human activities have contributed greatly to the emission of greenhouse gases (GHGs) to the atmosphere, especially carbon dioxide (CO<sub>2</sub>).<sup>1</sup> The main anthropogenic CO<sub>2</sub> emission is caused by the combustion of fossil fuels due to high demand of energy needed to produce electricity. According to the Environmental Protection Agency from the United States, up to 81% of the major gas emission of GHGs is occupied by CO<sub>2</sub> compared to the other minor gases such as methane, nitrous oxide and fluorinated gases.<sup>2</sup> Further, the Intergovernmental Panel on Climate Change (IPCC) has emphasised in their report that one of the broad elements of climatic change is the interaction of emissions, climate, risks and development pathways. The remaining carbon budget is limited to the long-term temperature limits between 1.5°C and 2°C.<sup>2</sup>

To achieve this goal, the emission of CO<sub>2</sub> must reduce. The CO<sub>2</sub> separation or sorption has become crucial as a potential approach. Membrane separation technology is one of the technologies that can solve the CO<sub>2</sub> emission by using the post combustion stage of CO<sub>2</sub> capture.<sup>3</sup>

Nevertheless, membrane formation normally includes a series of processes that rely on few parameters such as casting thickness. The effect of casting thickness during the membrane fabrication process has great impact on the membrane performance and structural transition as well as the coagulation step of immersion. The variation in structural transition affects the pore radius and the continuity of pores results in gas separation efficiencies.<sup>4</sup>

In addition, the fabrication of blend CAB membrane was investigated, with regards to its casting thickness. Cha and Jawad studied the casting thickness of CAB blend membranes from 150 μm–300 μm at equal ratios of CAB molecular weights of 12,000 and 65,000. They concluded that the highest CO<sub>2</sub> permeance of 106.87 ± 1.03 GPU and CO<sub>2</sub>/N<sub>2</sub> selectivity of 6.948 ± 0.081 for CAB blend membrane was synthesised at a casting thickness of 250 μm.<sup>5</sup>

The hydrophilic CAB blend of 12 wt%–15 wt% of acetyl content was studied and it was found that the more hydrophilic the membrane, the better the selectivity and the CO<sub>2</sub> permeance. This was due to the presence of polar function groups of hydroxyl and carboxyl, which could react with CO<sub>2</sub>.<sup>6</sup>

The Hansen solubility parameter (HSP) is useful in determining the compatibility of cellulose membranes. HSP is a tool for the preparation of emulsion and measures the miscibility of the mixture.<sup>7</sup> It is also used to investigate the adhesion in the interface of the solvent. By using HSP, the solubility of a polymer in a solvent or the compatibility of a polymer and plasticiser in a solvent dispersion can be found to be similar.<sup>7</sup> In Figure 1, the hydrogen ( $\delta_H$ ) and polar ( $\delta_P$ ) bond parameters are illustrated at different locations for common solvents<sup>8</sup> while the dispersion force (D), the polar force (P) and the hydrogen bonding force (H) are represented in Figure 2.<sup>9</sup>

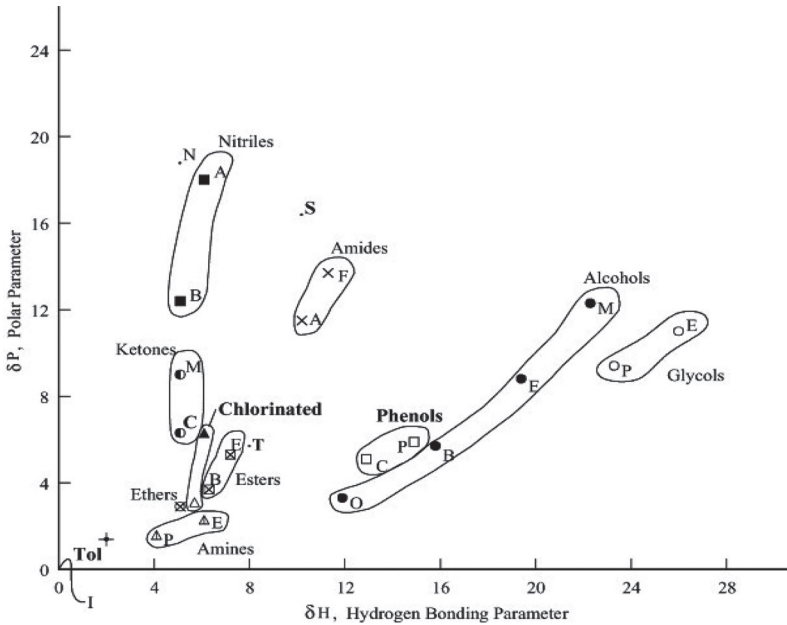


Figure 1: Hydrogen bond parameter ( $\delta_H$ ) and Polar bond parameter ( $\delta_P$ ) plot showing the location of various common solvents. The glycols are ethylene glycol (E) and propylene glycol (P). The alcohols are methanol (M), ethanol (E), 1-butanol (B) and 1-octanol (O). The amides include dimethyl formamide (F) and dimethyl acetamide (D). The nitriles are acetonitrile (A) and butyronitrile (B). The esters are ethyl acetate (E) and n-butyl acetate (B). The amines are ethyl amine (E) and propyl amine (P). The phenols are phenol (P) and m-cresol (C). The ethers are represented by diethyl ether. Bold type indicates relatively high  $\delta_D$ .<sup>8</sup>

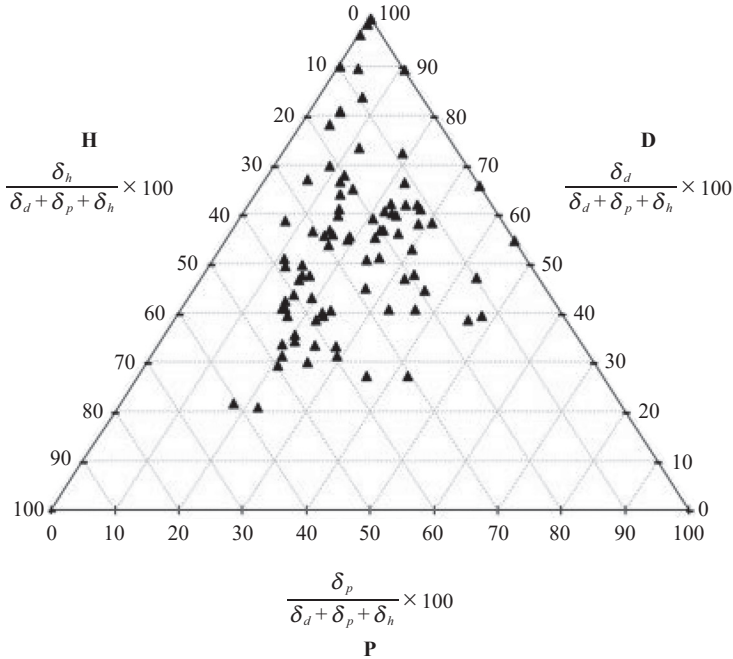


Figure 2: A triangular representation of the HSP where, D is the dispersion force, P is the polar force and H is the hydrogen bonding force where the point represents a common solvent.<sup>9</sup>

The aim of this work is to study the HSP, hydrophilicity and different casting thickness of blend CAB membrane, which is synthesised at molecular weights of 12,000:65,000:30,000 in the ratio of 1:2:2 towards CO<sub>2</sub>/N<sub>2</sub> separation. Up to date, no literature has been conducted on the understanding of the compatibility between the CAB polymer at molecular weights of 12,000:65,000:30,000 and the solvent (chloroform) of the new blend CAB membrane.

## 2. MATERIALS AND METHODOLOGY

### 2.1 Fabrication of Blend CAB Membranes

The blend CAB membrane was fabricated by using the wet-phase inversion method.<sup>5</sup> 4 wt% of CAB polymers (Sigma-Aldrich, Malaysia) were mixed in a ratio of 1:2:2 at molecular weight 12,000:30,000:65,000 with 96 wt% of chloroform (Merck, Malaysia) to fabricate the membrane. The solution was then stirred for a duration of 24 h until the CAB polymer dissolved fully in the solvent. After the stirring process, the well-mixed solution underwent sonication

for 20 min. This was to ensure that all the bubbles in the solution were eliminated completely as well as to ensure the surface homogeneity of the neat membrane.<sup>5</sup> A casting machine was then used to cast the membrane with casting thickness of 150  $\mu\text{m}$  (M1), 250  $\mu\text{m}$  (M2) and 300  $\mu\text{m}$  (M3), respectively. This was followed by solvent evaporation time of 5 min to ensure that all the solvent evaporated at room temperature.<sup>4</sup> Next, the membrane obtained was immersed for 24 h in distilled water at a temperature of 25°C to remove the solvent further. Thereafter, it was under sonification by using S60H Elmasonic (German) to remove the bubbles. The membrane formed was first immersed in isopropyl alcohol (Merck, Malaysia) for 1 h and then in n-hexane (Merck, Malaysia) for another 1 h. The fabricated membrane was placed in between filter papers and glass plates to dry for 24 h under room temperature. This ensured the evaporation of the remaining volatile liquid and subsequently stored for further use.<sup>4</sup>

## 2.2 Hansen Solubility Parameter (HSP)

The HSP is used to analyse the solubility of blend CAB polymer. The total energy of vaporisation can be calculated by the formula as shown in Equations 1 to 4.<sup>8</sup>

$$\% dTeas = \frac{\delta_d}{\delta_d + \delta_p + \delta_h} \times 100 \quad (1)$$

Group contribution method:

(a) Dispersion forces, D:

$$\delta_d = \frac{\sum F_d}{\sum V} \quad (2)$$

(b) Polar forces, P:

$$\delta_p = \frac{(\sum F_p^2)^{1/2}}{\sum V} \quad (3)$$

(c) Hydrogen bonding forces, H:

$$\delta_h = (\sum -U_m / \sum V)^{1/2} \quad (4)$$

$\delta_d$ ,  $\delta_p$  and  $\delta_h$  represent the dispersion, polar and hydrogen bond parameters, respectively. The locations of the common solvents relative to each other on a  $\delta_p$  versus  $\delta_h$  plot are shown in Figure 1. The parameters for the mixed solvents are found by volume, in addition to the respective parameters.<sup>8</sup>

The distance between the materials is defined as Ra, which is formulated in Equation 5.<sup>10</sup>

$$RA_{P-S} = \sqrt{(\delta_{d,P} - \delta_{d,S})^2 + (\delta_{p,P} - \delta_{p,S})^2 + (\delta_{h,P} - \delta_{h,S})^2} \quad (5)$$

Another useful parameter is the relative energy difference (RED), which is denoted by Ra divided by Ro. Ra is the largest value that is allowed for solubility. Meanwhile, Ro is the radius of the HSP sphere. The formula of RED is shown in Equation 6.<sup>10</sup> Figure 2 displays the ternary plot having a relative value for each HSP component. This ternary plot is used to estimate the HSP of blend CAB membrane.<sup>9</sup>

$$RED = Ra/Ro \quad (6)$$

## 2.3 Characterisation Studies of Blend CAB Membranes

### 2.3.1 Attenuated total reflectance fourier-transform infrared spectroscopy (ATR-FTIR)

This characterisation was performed to study the chemical properties of the fabricated membranes. The ATR-FTIR was done by using the Agilent Model: Cary 630. The spectrometer range was 400 cm<sup>-1</sup>–4,000 cm<sup>-1</sup>. The background wavenumber was recorded prior to the wave numbers of the samples. Data was collected with 32 scans using resolution of 4 cm<sup>-1</sup> setting through the diamond crystal.<sup>11</sup>

### 2.3.2 Surface contact angle

The wettability of the fabricated membrane was studied by measuring the surface contact angle with the Drop Shape Analyser: Model DSA 100B. Ten readings were taken and recorded for analysis.<sup>12</sup>

## 3. RESULTS AND DISCUSSION

### 3.1 HSP

Figure 3 represents the HSP of blend CAB membrane by using the graphical method where HSP of the CAB membrane can be estimated. In the ternary HSP diagram, three components of HSP are used as reference axes in the diagram. The three axes represent the values of dispersion, polarity and hydrogen bonding components of the HSP of a compound in percentages.<sup>13</sup> The sum of the three forces is 100%.

Table 1 summarises the HSP of solvents and HSP of solutes by the group contribution method. By using this method, the membrane solubility parameters can be calculated relatively easily. The closer the HSP values of solvent and solute, the better the solvent is for that solute.<sup>14</sup> From this graphical method shown in Figure 3, the HSP value of CAB, chloroform, isopropyl alcohol and n-hexane are located on the same diagonal, which proves the good compatibility among polymer, solvent and drying exchange-solvents in the blend CAB membrane. When the affinity is high among the solvent and the particles, it indicates the well-dispersion and the low-sedimentation rate.<sup>15</sup>

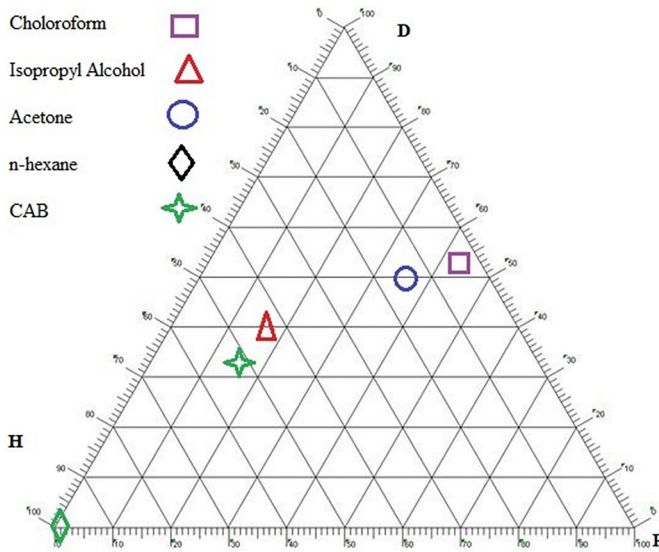


Figure 3: HSP of membranes by graphical method.

## 3.2 Effect of Casting Thickness

### 3.2.1 FTIR

As displayed in Figure 4, the ATR-FTIR spectra of the blend CAB membranes with casting thickness of 150  $\mu\text{m}$  (M1), 250  $\mu\text{m}$  (M2) and 300  $\mu\text{m}$  (M3) are plotted. Absorbance is used for the y-axis to ease the quantitative comparison between the membrane. This is because it is directly related to the concentration based on the Beer-Lambert's Law. Membranes M1 to M3 shows a strong stretching band around 1,044.07  $\text{cm}^{-1}$  and 1,226.25  $\text{cm}^{-1}$  indicating the presence of single bond C-O stretching while the peak around 1,161.56  $\text{cm}^{-1}$  shows the aliphatic ether (C-O-C). Furthermore, there is also strong stretching vibration at 1,744.04  $\text{cm}^{-1}$  due to the presence of the carbonyl (C=O) group. Besides that,

Table 1: Summary of HSP of solvents, HSP of solute by group contribution method.

Solvents	$\delta_d$	$\frac{\delta_d}{\delta_d + \delta_p + \delta_h} \times 100$	$\delta_p$	$\frac{\delta_p}{\delta_d + \delta_p + \delta_h} \times 100$	$\delta_h$	$\frac{\delta_h}{\delta_d + \delta_p + \delta_h} \times 100$	$\delta_d + \delta_p + \delta_h$
	MPA <sup>0.5</sup>	%	MPA <sup>0.5</sup>	%	MPA <sup>0.5</sup>	%	MPA <sup>0.5</sup>
Chloroform	17.85	53.00	14.01	41.85	1.66	5.15	33.55
Isopropyl alcohol	14.87	39.47	6.58	17.50	16.22	43.03	37.67
Acetone	14.52	49.23	9.90	33.57	5.07	17.20	29.89
n-hexane	14.61	100.00	0.00	0.00	0.00	0.00	14.61
CAB	20.04	33.00	9.59	15.79	31.10	51.21	60.73



the small peak is due to C-H stretching. Meanwhile, a broad peak around  $3,545.45\text{ cm}^{-1}$  is due to the hydroxyl (O-H) group. Although  $\text{N}_2$  molecules are non-polar and less polarised than  $\text{CO}_2$ , they are still capable of interacting weakly with the carbonyl (C=O) group by utilising their  $\pi$ -electron system.<sup>16</sup> Hence, when the C=O stretch intensity increases with casting thickness, the amount and strength of C=O group increases as well. This leads to the intermolecular interactive force with the  $\text{N}_2$  molecules, which strengthens the C=O groups and enhances the gas solubility in the dense film.<sup>5</sup> Therefore, the  $\text{N}_2$  capture is higher in a thicker membrane. Thus, M3 has the lowest  $\text{N}_2$  permeance with a higher casting thickness.

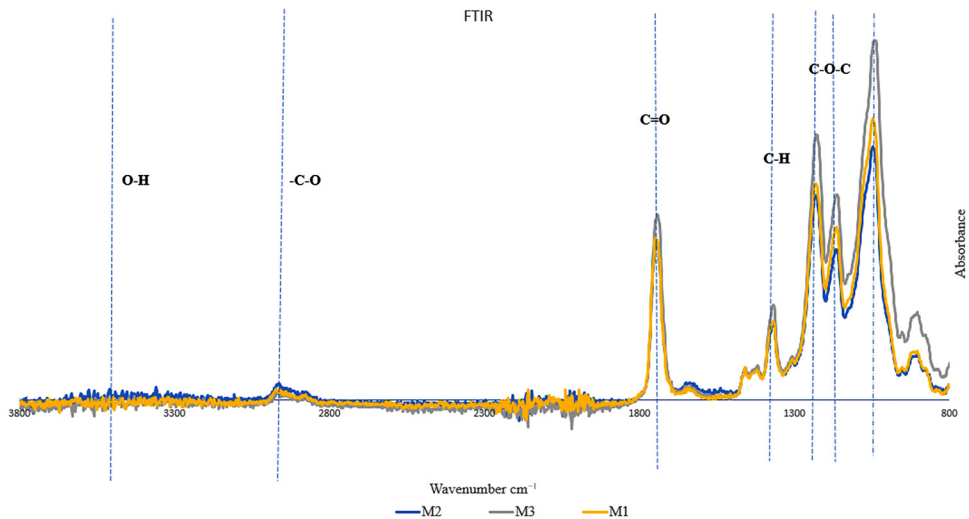


Figure 4: FTIR for blend CAB membranes synthesised with various casting thickness of  $150\text{ }\mu\text{m}$ ,  $250\text{ }\mu\text{m}$  and  $300\text{ }\mu\text{m}$  for M1, M2 and M3, respectively, which are casted with solvent evaporation time of 5 min at different pressures. The spectra are presented in offset appearance for better visibility.

According to the study by Manimaran et al., the experiment conducted studied the effects of solvent evaporation time and casting thickness on the gas separation performance of blend CAB membrane.<sup>11</sup> This is based on the ATR-FTIR spectra generated in Figure 5, which shows the rich carbonyl (C=O) and hydroxyl (O-H) groups in the CAB membrane. Both C=O and O-H are considered high polar functional groups. Thus, this can greatly affect the gas separation performance. With the increase in polar functional groups, the selectivity of the membrane is improved.<sup>11</sup> Another study conducted by Chong et al. in the year 2020, studied the molecular weights of blend CAB membrane for  $\text{CO}_2/\text{N}_2$  separation.<sup>12</sup> As shown in Figure 6 and based on the findings of the ATR-FTIR spectra generated,

M3 consists of the higher polar functional group (-OH) when compared to M2. M2 and M3 are fabricated with different molecular weights of 12,000, 70,000 and 30,000 in the ratios of 1:1:0 and 1:2:0, respectively. The selectivity of M3 and M2 is increased in the ratio of 1:2. The results indicate that with the presence of the higher polar functional groups, the selectivity of the membranes is enhanced. Furthermore, Yong and Zhang proved that the functional groups of the CAB polymer have higher interaction with the CO<sub>2</sub> molecules.<sup>17</sup> The blend CAB membrane illustrated the same ATR-FTIR spectra, indicating that it consists of high polar functional groups based on the spectra generated such as carbonyl (C=O) and hydroxyl (O-H) groups. As a result, this affects the membrane gas separation performance. Hence, by comparing these previous researches, the blend CAB membrane is proven as one of the methods that enhances the membrane gas separation performance with similar functional groups as exhibited in the membrane. In conclusion, the characterisation of the CAB polymer membrane using ATR-FTIR, results in high polar functional groups such as carbonyl (C=O) and hydroxyl (O-H). The higher the polar functional groups, the higher the selectivity of the fabricated membrane for CO<sub>2</sub>/N<sub>2</sub>.

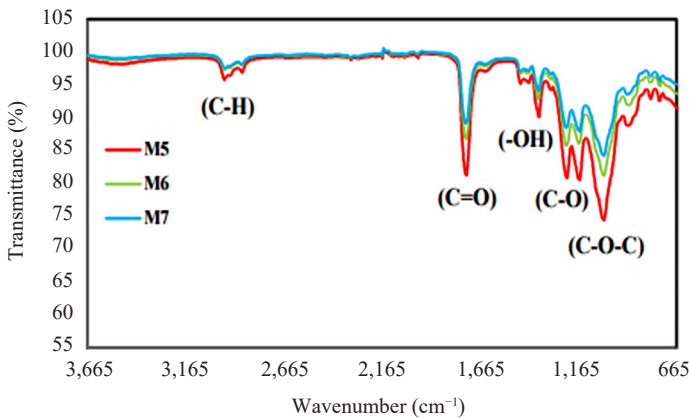


Figure 5: ATR-FTIR spectroscopy for CAB membrane fabricated with different range of casting thickness and solvent evaporation time of 4.5 min.<sup>11</sup>

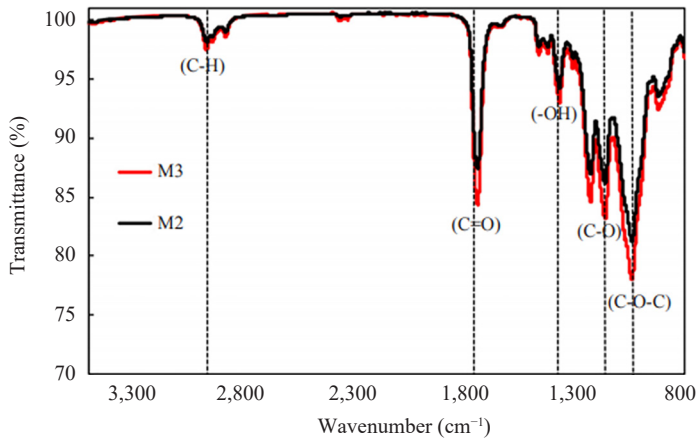


Figure 6: ATR-FTIR spectra of CAB membrane with 250  $\mu\text{m}$  casting thickness and 5 min solvent evaporation time respectively.<sup>12</sup>

### 3.2.2 Contact angle

With reference to Figure 7, the contact angles for M1, M2 and M3 are  $120.46^\circ$ ,  $92.95^\circ$  and  $71.42^\circ$ , respectively. Membrane casting thickness increases directly proportionally to contact angle decreases, thus, increasing the hydrophilicity. Having a high contact angle indicates the hydrophobic nature of the membrane surface. When the value is greater than 90, the affinity between the water and surface reduces, meaning that the hydrophilicity is lower.<sup>18</sup> The increase in hydrophilicity is mainly due to the higher presence of hydrophilic groups like C=O and O-H in the membrane. As hydrophilicity increases, the strength of the dipole-quadrupole interaction between the polar O=H group and non-polar  $\text{CO}_2$  gas molecules increases, resulting in the membrane's strong affinity for  $\text{CO}_2$  molecules. This leads to decrease in the rate of  $\text{CO}_2$  flowing through the membrane, thus, resulting in a trend that reduces the O permeance through the membrane.<sup>4</sup>

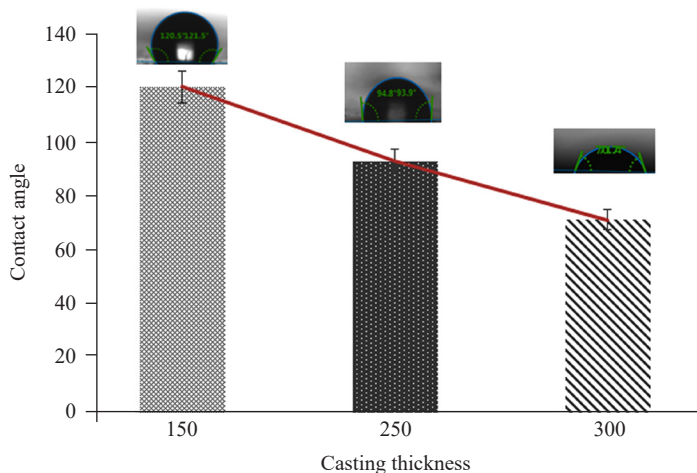


Figure 7: Contact Angles for blend CAB membranes synthesised with various casting thickness of 150 μm, 250 μm and 300 μm for M1, M2, and M3, respectively, which are casted with solvent evaporation time of 5 min at different pressures.

### 3.2.3 Membrane performance test

#### 3.2.3.1 CO<sub>2</sub> permeance

The membrane separation performance can be determined through single gas permeation tests. Tests for the fabricated membranes M1, M2 and M3 with various casting thickness of 150 μm, 250 μm and 300 μm, respectively, at solvent evaporation time of 5 min and different pressures were conducted to determine the performance. With reference to Figure 8, the CO<sub>2</sub> permeance for blend CAB membranes M1, M2 and M3 are found to be  $10294.75 \pm 26$  GPU,  $7560.80 \pm 20$  GPU and  $5906.40 \pm 19$  GPU, respectively. M1 has the highest CO<sub>2</sub> permeance performance amongst all at  $10294.75 \pm 26$  GPU. Overall, the CO<sub>2</sub> permeance of the membranes decreased as the casting thickness increased. This is because of the increase in hydrophilicity when the casting thickness increases. As shown in Figure 7, M1 has the higher contact angle at  $120.46^\circ$  compared to M2 and M3, which have contact angles of  $92.95^\circ$  and  $71.42^\circ$ , respectively. This is because the contact angles decrease with increase in casting thickness resulting in increase of hydrophilicity. The high hydrophilicity in M1 is due to the higher presence of polar functional groups such as carbonyl (C=O) and hydroxyl (O-H) as discussed in the ATR-FTIR section. As hydrophilicity increases, the strength of the dipole-quadrupole interaction between the polar O-H group and non-polar CO<sub>2</sub> gas molecules increases as well, resulting in the membrane's strong affinity for CO<sub>2</sub> molecules.<sup>19</sup>

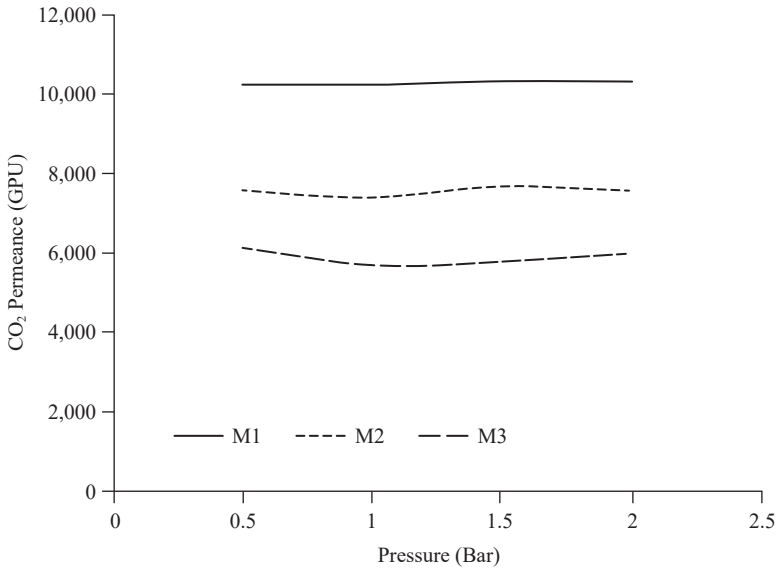


Figure 8: CO<sub>2</sub> Permeance for blend CAB membranes synthesised with various casting thickness of 150  $\mu\text{m}$ , 250  $\mu\text{m}$  and 300  $\mu\text{m}$  for M1, M2 and M3, respectively, which are casted with solvent evaporation time of 5 min at different pressures.

### 3.2.3.2 N<sub>2</sub> permeance

Figure 9 shows the N<sub>2</sub> gas permeance for blend CAB membranes M1, M2 and M3, which are 9,581.75  $\pm$  21 GPU, 7,601.08  $\pm$  18 GPU and 5,823.10  $\pm$  22 GPU, respectively. Similar with CO<sub>2</sub> permeance, M1 exhibits the highest N<sub>2</sub> permeance performance at 9,581.75  $\pm$  21 GPU. Further, the N<sub>2</sub> permeance decreases with increase in casting thickness. This is mainly due to the increase of the carbonyl group as the thickness increases. Based on Figure 4, a strong stretching vibration at 1,744.04  $\text{cm}^{-1}$  is observed due to the presence of the carbonyl (C=O) group. Therefore, this induces the intermolecular interactive force between the N<sub>2</sub> molecules and C=O, which strengthens and enhances the gas solubility in the dense film. Thus, N<sub>2</sub> in the membrane, subsequently increases the mass transfer of N<sub>2</sub>, which causes tougher permeation of gas through the membrane.<sup>16</sup> Therefore, M3 has the lowest N<sub>2</sub> permeance with the highest casting thickness.

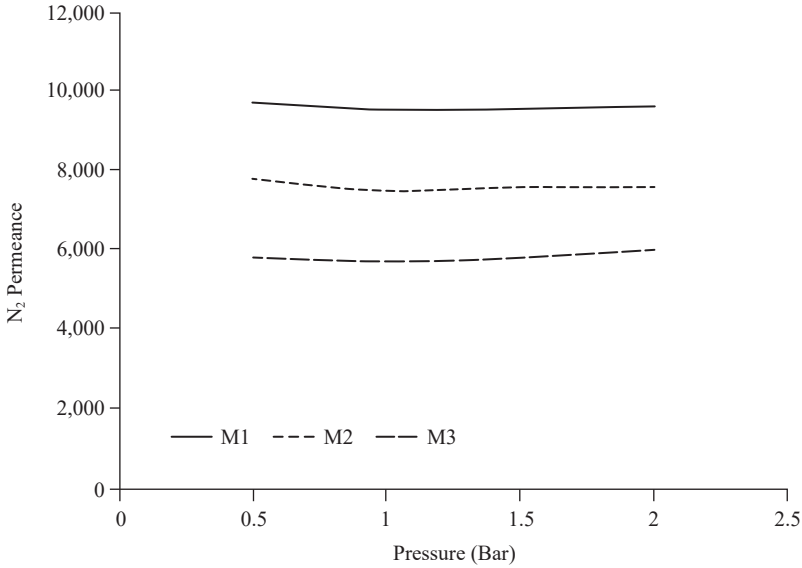


Figure 9: N<sub>2</sub> Permeance for blend CAB membranes synthesised with various casting thickness of 150  $\mu\text{m}$ , 250  $\mu\text{m}$  and 300  $\mu\text{m}$  for M1, M2 and M3, respectively, which are casted with solvent evaporation time of 5 min at different pressures.

### 3.2.3.3 CO<sub>2</sub>/N<sub>2</sub> selectivity

As shown in Figure 10, the CO<sub>2</sub>/N<sub>2</sub> selectivity for the blend CAB membranes (M1, M2 and M3) are approximately  $0.9369 \pm 0.03$ ,  $1.5319 \pm 0.05$  and  $1.0962 \pm 0.05$ , respectively. Amongst these membranes, M2 shows the highest selectivity. Meanwhile, M1 and M3 shows similar selectivity. The selectivity of M2 increases because of the insignificant reduction in CO<sub>2</sub> permeance when compared to N<sub>2</sub>. This is because the contact angle decreases when there is a small difference in the hydrophilicity of M2 and M3. Furthermore, the strong interacting force between the membranes and CO<sub>2</sub> permeance also results in a significant increasing trend of the strength of the CO<sub>2</sub>-philic functional group. The CO<sub>2</sub> permeance reduces slowly when compared to the N<sub>2</sub> permeance as indicated in Figures 8 and 9. This is because the high polar group increases the stronger interacting force between the membranes and the CO<sub>2</sub> molecules. These high polar groups are C=O, O-H and C-O-C when the spectra peak increases, as illustrated in Figure 4. The decrease in contact angles from 92.95° to 71.42° indicates a huge difference in hydrophilicity from M2 to M3.

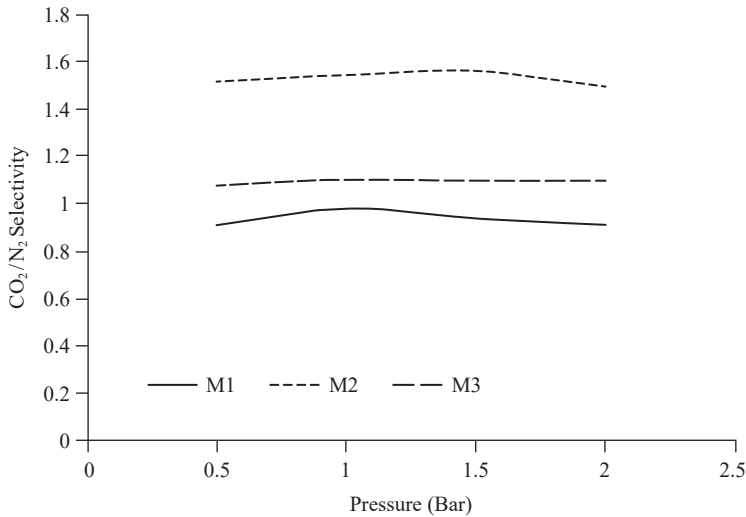


Figure 10:  $\text{CO}_2/\text{N}_2$  Selectivity for blend CAB membranes synthesised with various casting thickness of 150  $\mu\text{m}$ , 250  $\mu\text{m}$  and 300  $\mu\text{m}$  for M1, M2 and M3, respectively, which are casted with solvent evaporation time of 5 min at different pressures.

In summary, both the  $\text{CO}_2$  and  $\text{N}_2$  permeance decrease with increase casting thickness while the  $\text{CO}_2/\text{N}_2$  selectivity increases from M1 and M2 to M3. Thus, the best casting selectivity is M2 with casting thickness of 250  $\mu\text{m}$ . Hence, M2 exhibits the best membrane with better performance among all the membranes due to its relatively high  $\text{CO}_2$  gas permeance and the highest  $\text{CO}_2/\text{N}_2$  selectivity.

#### 4. CONCLUSION

In this study, the blend CAB membranes were fabricated utilising the wet-phase inversion method. The blend CAB membranes were also fabricated with molecular weights of 12,000, 30,000 and 65,000 in the ratio of 1:2:2 at different casting thicknesses. Based on the characterisation using the ATR-FTIR, it was clear that the CAB polymer membranes showed that the higher the polar functional groups, the higher the selectivity of the fabricated membranes. The  $\text{CO}_2/\text{N}_2$  selectivity was  $1.5319 \pm 0.05$  and the  $\text{CO}_2$  gas permeance was  $7560.80 \pm 20$  GPU.

#### 5. ACKNOWLEDGEMENTS

The authors would like to thank Qatar University on providing the international research collaboration co-fund (IRCC) with award number CENG-IRCC-2023-110.

## 6. REFERENCES

1. The Intergovernmental Panel on Climate Change (IPCC). (2020). *AR6 Synthesis Report: Climate Change 2022*. IPCC.
2. Environmental Protection Agency (EPA). (2020). *Overview of greenhouse gases*. United States Environmental Protection Agency.
3. Brunetti, A. et al. (2010). Membrane technologies for CO<sub>2</sub> separation. *J. Memb. Sci.*, 359(1–2), 115–125. <https://doi.org/10.1016/j.memsci.2009.11.0404>.
4. Lee, R. J. et al. (2020). Blend cellulose acetate butyrate/functionlised multi-walled carbon nanotubes mixed matrix membrane for enhanced CO<sub>2</sub>/N<sub>2</sub> separation with kinetic sorption study. *J. Environ. Chem. Eng.*, 8(5), 104212. <https://doi.org/10.1016/j.jece.2020.104212>
5. Cha, W. C. & Jawad, Z. A. (2019). The influence of cellulose acetate butyrate membrane structure on CO<sub>2</sub>/N<sub>2</sub> separation: Effect of casting thickness and solvent exchange time. *Chem. Eng. Commun.*, 207(4), 474–492. <https://doi.org/10.1080/00986445.2019.1605359>
6. Lee, R. et al. (2018). Incorporation of functionalized multi-walled carbon nanotubes (MWCNTs) into cellulose acetate butyrate (CAB) polymeric matrix to improve the CO<sub>2</sub>/N<sub>2</sub> separation. *Proc. Safety Environ. Prot.*, 117, 159–167. <https://doi.org/10.1016/j.psep.2018.04.0217>
7. Johannes, K. F. (2012). Dispersion, emulsions and foams. In K. F., Johannes. (Ed.). *Petroleum engineer's guide to oil field chemicals and fluids*. 663–694. <https://doi.org/10.1016/B978-0-12-383844-5.00021-0>
8. Hansen, C. M. (2007). Hansen solubility parameter: A user's handbook, 2nd ed. Boca Raton: CRC Press. <https://doi.org/10.1201/9781420006834>
9. Saiz, C. A. et al. (2017). Shortcut application of the Hansen solubility parameter for organic solvent nanofiltration. *J. Memb. Sci.*, 546, 120–127. <https://doi.org/10.1016/j.memsci.2017.10.016>
10. Charles, M. H. (2004). 50 years with solubility parameter- past and future. *Prog. in Org. Coat.*, 51(1), 77–84. <https://doi.org/10.1016/j.porgcoat.2004.05.004>
11. Manimaran, D. et al. (2019). Effect of solvent evaporation time and casting thickness on the separation performance of cellulose acetate butyrate blend membrane. *J. Appl. Mem. Sci. Technol.*, 23(2), 11–22. <https://doi.org/10.11113/amst.v23n2.151>
12. Chong, D. S. et al. (2020). The influence of blending different molecular weight of cellulose acetate butyrate for CO<sub>2</sub>/ N<sub>2</sub> separation. *J. Phys. Sci.*, 31(2), 91–112. <https://doi.org/10.21315/jps2020.31.2.7>
13. Mihalovits, M. (2022). Determination of the Hansen solubility parameters from solubility data using an improved evaluation approach, the concentric spheroids method. *J. Mol. Liq.*, 364, 119911. <https://doi.org/10.1016/j.molliq.2022.119911>
14. Carlos, et al. (2018). Shortcut applications of the Hansen solubility parameter for organic solvent nanofiltration. *J. Memb. Sci.*, 546, 120–127. <https://doi.org/10.1016/j.memsci.2017.10.016>



15. Tsutsumi, S. et al. (2019). Determination of Hansen solubility parameters of particles using a capillary penetration method. *Chem. Phys.*, 521, 115–122. <https://doi.org/10.1016/j.chemphys.2019.01.018>
16. Blatchford, M. A. (2003). Spectroscopic studies of model carbonyl compounds in CO<sub>2</sub>: Evidence for cooperative C–H–O interactions. *J. Phys. Chem. A*, 107(48), 10311–10323. <https://doi.org/10.1021/jp027208m>
17. Yong, W. F. & Zhang, H. (2020). Recent advances in polymer blend membranes for gas separation and evaporation. *Prog. Mater. Sci.*, 116, 100713. <https://doi.org/10.1016/j.pmatsci.2020.100713>
18. Hebbar, R. S. et al. (2017). Contact angle measurements. *Membr. Charac.*, 219–255. <https://doi.org/10.1016/B978-0-444-63776-5.00012-7>
19. Lin, K. Y. A. & Park, A. H. A. (2011). Effects of bonding types and functional groups on CO<sub>2</sub> capture using novel multiphase systems of liquid-like nanoparticle organic hybrid materials. *Environ. Sci. Technol.*, 45(15), 6633–6639. <https://doi.org/10.1021/es200146g>